This is the author's version of an article that has been published in IEEE.
The final version of record is available at https://doi.org/10.1109/ICC42927.2021.9500351

On COVID-19 Prediction Using Asynchronous Federated Learning-Based Agile Radiograph Screening Booths

Sadman Sakib*[1], Mostafa M. Fouda†[2], Zubair Md Fadlullah*‡[3], and Nidal Nasser§[4].
*Department of Computer Science, Lakehead University, Thunder Bay, Ontario, Canada.
†Department of Electrical and Computer Engineering, Idaho State University, Pocatello, ID, USA.
‡Thunder Bay Regional Health Research Institute (TBRHRI), Thunder Bay, Ontario, Canada.
§College of Engineering, Alfaisal University, KSA.
Emails: [1]ssak2921@lakeheadu.ca, [2]mfouda@ieee.org, [3]zubair.fadlullah@lakeheadu.ca, [4]nnasser@alfaisal.edu.

***Abstract*—To combat the novel coronavirus (COVID-19) spread, the adoption of technologies including the Internet of Things (IoT) and deep learning is on the rise. However, the seamless integration of IoT devices and deep learning models for radiograph detection to identify the presence of glass opacities and other features in the lung is yet to be envisioned. Moreover, the privacy issue of the collected radiograph data and other health data of the patients has also arisen much concern. To address these challenges, in this paper, we envision a federated learning model for COVID-19 prediction from radiograph images acquired by an X-ray device within a mobile and deployable screening resource booth node (RBN). Our envisioned model permits the privacy-preservation of the acquired radiograph by performing localized learning. We further customize the proposed federated learning model by asynchronously updating the shallow and deep model parameters so that precious communication bandwidth can be spared. Based on a real dataset, the effectiveness of our envisioned approach is demonstrated and compared with baseline methods.**

***Index Terms*—X-ray, federated learning, COVID-19, IoT.**

I. Introduction

As the second wave of the novel coronavirus disease, commonly referred to as COVID-19, continues to emerge in various parts of the world, the need to design effective interdisciplinary approaches has become paramount to thwart the onslaught of the pandemic. Thus, medical analytics coupled with the Internet of Things (IoT) and mobile edge computing are gaining significant momentum, paving the way for tactile sensing [1], haptic communication [2], augmented and virtual reality [3], and so forth, to combat COVID-19. While the reverse transcription-polymerase chain reaction (RT-PCR) is recognized as the gold standard for COVID-19 diagnostics [4], medical experts are exploring additional modalities to complement the detection of COVID-19. Indeed, additional modalities can provide a finer resolution of information to deduce non-asymptomatic individuals, track the progress of COVID-19 severity in vital organs, and so forth [5]. For example, patients having risk factors for COVID-19 progression, chest radiograph such as X-ray, along with clinical symptoms, may indicate whether to follow home-isolation or to refer to secondary care [4].

While radiograph analytics-based COVID-19 detection with high accuracy was investigated in our earlier work with a combination of a customized generative adversarial network (GAN) and convolutional neural network (CNN) models in [5], a key concern for users' medical data privacy is yet to be addressed in the existing literature. Despite data anonymization techniques, the cloud servers (where preprocessing and training of these models takes place) could reveal sensitive information regarding the patients under various security threats [6]. In this paper, we take into account the patients' privacy concern in the use-case of COVID-19 radiograph data acquisition and investigate how to carry out a distributed learning without the need for explicit data sharing with the cloud. In this vein, as depicted in Fig. 1, we aim to develop an agile data acquisition system for radiograph for COVID-19 detection with mobile and deployable resource booth nodes (RBNs) acting as edge computing nodes. An RBN can be scheduled to visit a remote or rural community and monitor a number of patients in a COVID-19 hotspot. The RBN is assumed to be a trusted node as it is physically supervised by public health personnel who do not have physical access to the radiograph images obtained by the

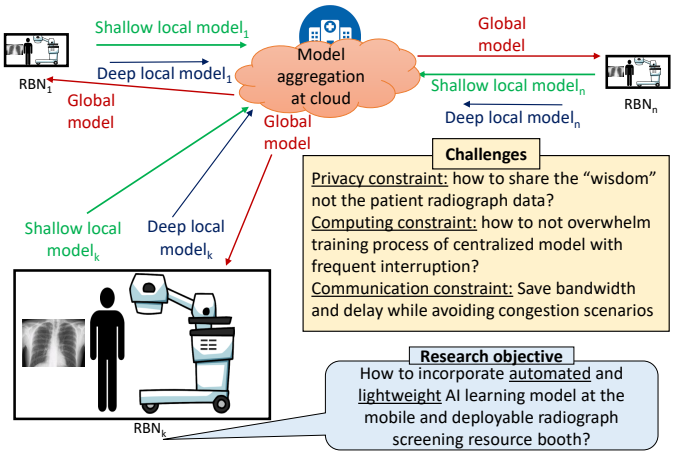

Fig. 1: System model: our main focus is to develop an agile, asynchronously updated federated learning-based X-ray analytic methodology at the distributed resource booth nodes (RBNs) to combat COVID-19 while preserving patient-data privacy.

device and the connectivity with the Internet with the RBN is physically disabled until the training algorithm improves the localized AI model for COVID-19 prediction from radiograph data leveraging our earlier technique in [5], and then securely deletes the data files. Upon updating its local AI model, the RBN shares the data with neighboring RBNs and the cloud by efficiently scheduling the shallow and deep parameters to reduce the communication overhead. By employing this unique concept of asynchronously updating AI model parameters of the RBNs, the privacy of the acquired medical data and network efficiency are jointly preserved. Using extensive experiments based on a publicly available robust dataset, we elucidate the effectiveness of the performance of our proposal.

The remainder of the paper is organized as follows. Section II surveys the relevant research work on combating COVID-19 with AI techniques. Our considered system model is discussed in section III. The formal problem is described in section IV. Next, our proposed asynchronously updating federated learning algorithm is presented in section V. The performance of our proposal is evaluated in section VI. Finally, section VII concludes the paper.

II. Related Work

For clarity, we segment the relevant research work into two categories: imaging modalities for diagnosing COVID-19 and AI-based analytics of chest images.

With the second wave of COVID-19 already emerging, many countries have scrambled their resources to better understand and diagnose the disease with as much information as possible. Radiology departments are active in tracking patients with COVID-19 manifestations in the lungs exhibiting flu-like features, particularly during the onset of the flu season to commence in the northern hemisphere this winter [7]. The work in [8] studied the similarity of COVID-19 with other coronavirus variants, including SARS (severe acute respiratory syndrome) and MERS (middle east respiratory syndrome), and indicated the importance of early chest imaging for combating COVID-19. Furthermore, the differentiation of bilateral nodular and peripheral glass opacities in lung imaging due to COVID-19 was discussed in [9].

On the other hand, AI-based radiograph analytics has emerged as a hot research area as indicated in the work in [10]–[12]. The DarkCovidNet model [13] employed CNNs to perform binary and multi-class classification involving normal, COVID-19, and pneumonia samples. Further improvement was obtained with jointly customized GAN and CNN models to automate COVID-19 detection in our earlier work in [5] demonstrating its superior performance over existing CNN models, including AlexNet, ResNet-18, ResNet-50, ResNet-101, SqueezeNet, VGG-16, VGG-19, MobileNet-V2, GoogleNet, and XceptionCT. However, admittedly, none of the aforementioned analytics methodologies took into account the patients' privacy requirement who are subject to contributing lung imaging data to hospitals and clinics that may end up in public health repositories. While data anonymization is done in preparing such public repository datasets, malicious attacks may be launched during the preprocessing or training stages of the AI model in the cloud [6]. This privacy concern implies the urgency to investigate a new learning technique without the need for sharing the image data explicitly with the cloud. While federated learning has emerged as a new learning paradigm [14], to the best of our knowledge, it has not yet been applied to design a pandemic response network due to the network overhead issues.

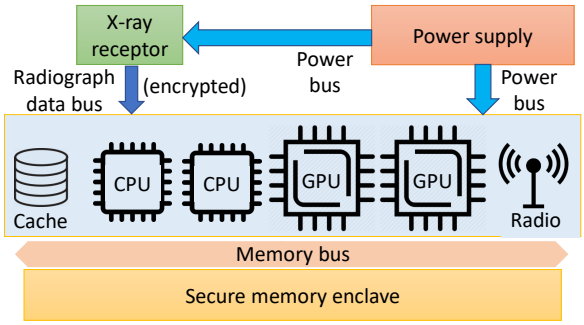

Fig. 2: System model: our main focus is to develop an agile, asynchronously updated federated learning-based X-ray analytic methodology at the distributed resource booth nodes (RBNs) to combat COVID-19 while preserving patient-data privacy.

III. Considered RBN System Model and Problem Description

In this section, we describe our considered mobile and deployable RBN system model inspired by existing prototypes [15]. Each RBN is assumed to consist of the radiograph component (i.e., X-ray sensor, receptor, tube, and so forth) and the necessary image conversion system to seamlessly digitize the acquired image as depicted in the high-level architecture of Fig. 2. With a cross-armed CCD camera, X-ray tube, and fixed diaphragms with a light localizer, a spatial resolution from 3 to 5 LP/mm (line pairs per millimeter) is possible radiograph acquisition. The cross-arm can move in a vertical direction to 1100 mm to accommodate variable heights of patients, and it can also rotate within a range of -90 to +90 degrees. Onboard the truck, a high-frequency generator is connected to a 220 V ± 10% electric system with a resistance of 1 Ohm to power up the X-ray components to satisfy its high power requirement. Also, as shown in Fig. 2, a secure memory enclave is used, which securely operates on the acquired radiograph images and take advantage of a pool of computing resources such as CPUs and GPUs. Once the secure computing is done, the computed model can be stored encrypted in the cache. The radio unit, capable of operating in multiple frequency bands supporting 4G and 5G mobile communications, provides connectivity to the cloud and neighboring RBNs servicing users nearby. For the truck-mounted RBN, we consider a waiting room for up to two patients to prepare prior to chest X-ray acquisition. In the screening room, the X-ray equipment is considered to be with sufficient shielding for safety purposes. Note that this system model based on mobile and deployable RBNs is supposed to

avoid possible safety issues [16] emanating from using portable X-ray machines at home by individual users. Also, the clinical grade X-ray equipment at the RBN means that high-resolution radiographs can be obtained, which is not possible with low-powered, hand-held X-ray devices that recently emerged in the market [16]. The secure enclave is considered to ensure the trustworthiness of the RBN so that the user's data are not tampered with or illegitimately duplicated or accessed. To enforce the notion of trust, the RBN is assumed to be managed by public health authority appointed personnel with appropriate credentials. With remote attestation with the public health authority server, the credential of the RBN manager (i.e., the designated personnel), and the secret information of the secure enclave, a secure radiograph data acquisition session is assumed possible. In addition, there is a physical switch that the RBN manager can enable or disable in conjunction with a software-driven contextual switch orchestrated by our proposed algorithm to be described in section V. Furthermore, the RBN unit is assumed to comprise no storage interfaces to copy the RBN cache's content trivially. Thus, the considered system model provides a trusted environment for radiograph data acquisition and computing to ensure that the patient data are not wrongfully accessed or acquired.

IV. Problem Description

The RBNs have the potential to extend service coverage for patients, particularly residing in remote/rural or difficult-to-access locations and pandemic-affected sites. Even though we considered only the radiograph collection use-case in the system model presented in section III, a myriad of data such as temperature, heartbeat, blood oxygen saturation, travel history, and so forth could be collected directly at the RBN or through IoT-enabled mobile applications. Each RBN then needs to provide a snapshot of the pandemic progression at a neighborhood level, while multiple RBNs can provide district-level information on how the pandemic is advancing. Thus, the first challenge is how to facilitate distributed learning among the RBNs. The second challenge consists of the user requirement for privacy as they typically are not willing to share the raw data with the cloud to avoid potential privacy breaches. The RBN also needs to ensure that their acquired data are securely used in the secure enclave and then deleted after a localized decision making (i.e., local model) is carried out. Thus, the RBNs require a distributed methodology to learn pandemic features (e.g., COVID-19 symptoms, pneumonia classification using radiographs, and so forth) with privacy preservation to maximize the learning accuracy. Because the RBNs lack a global view of patients spread over a wide geographical area, how they may perform decentralized machine learning without sharing the raw health data of the users arises a challenge. In this vein, the RBNs could form a federation to learn these information among themselves. RBNs could also exchange the information with the cloud to further boost the decentralized training among them. Upon receiving the locally trained models at the RBN layer, the cloud can then train a global model to arrive at an optimized COVID-19 prediction with significantly high accuracy. In other words, the objective is to minimize a loss function:

$$min \sum_{i=1}^{N} \frac{\mathcal{S}_i}{\mathcal{S}} f_i(w, x_k, y_k), \tag{1}$$

where $f_i(w, x_k, y_k)$, $\mathcal{S}_i$, and $\mathcal{S}$ denote the loss function of RBN_i, the sample size (locally monitored/acquired health data) of RBN_i, and the training samples used by the cloud, respectively. Each RBN consists of a weight vector, w, which represents its locally trained AI model parameters using x_k and y_k. The value of $f_i(w, x_k, y_k)$ increases with the growing prediction error $(x_k^{\intercal} w - y_k)$. Therefore, the constraint $w_1 = w_2 = ... = w_k$ is needed to guarantee the convergence of global learning such that all RBNs and the cloud can eventually derive the same AI model without explicitly exchanging the raw health data of the patients.

To summarize, the research challenge is to design a technique so that (1) each RBN is capable of training a shared global model with its local model update based on its data, and (2) each RBN shares its updated local model with the neighboring RBNs and the cloud to revise/update the global model. Until the loss function is minimized and/or the global model accuracy is deemed reasonable, this distributed training process needs to continue. Therefore, designing such a decentralized technique with reduced network overhead and privacy-preservation property can be regarded as the primary research problem of our work in this paper.

V. Proposed Deep Learning-Based Algorithm

In this section, we present our envisioned asynchronous federated learning model for privacy-preserving COVID-19 screening. Our methodology hinges upon Algorithms 1 and 2. Note that the global and local AI models, constructed at the cloud and RBNs, respectively, are facilitated by either a custom ANN (artificial neural network) model or a customized CNN model. Both these deep learning models were conceptualized in our earlier work in [5] for a centralized COVID-19 prediction.

Algorithm 1 accepts the set of all available RBNs, denoted as RBN, and it returns the trained global model characterized as M_g. Step 1 of this algorithm is the initialization phase. In steps 5 to 7, the set of all RBNs is traversed, and the transmitted parameters are aggregated and sent back to the RBNs. The learning performance of the model is accessed in step 8 and compared with the threshold (min_{loss}). The learning phase at the cloud runs until the loss is less than or equal to the pre-defined threshold.

The algorithm that runs on the RBN's side is exhibited in Algorithm 2. The phase commences with the inputs u, Δ, T, and λ. The details of these inputs are manifested in the algorithm's input segment. From step 1 to 3, the required parameters related to the algorithm and the local model (M_u) is initialized with selected values. In step 4, the software-driven contextual switch flag (cs_u) is initialized as false. The adopted data size of each radiograph data is determined in step 5. Here, the radiograph data's row and column size are initialized as d_r

Algorithm 1: Central aggregated asynchronous learning at cloud

Input : RBN (set of all RBNs), min_{loss} (performance threshold)
Output: M_g (global trained model)

1 $M_g \leftarrow \emptyset$
2 **while** *true* **do**
3 **for** u=*1 to* $length(RBN)$ **do**
4 update M_g by aggregating the received parameters (W_u) from RBN_u
5 **end**
6 $curr_{acc} \leftarrow$ access the current performance of global model M_g
7 **if** *(*$curr_{loss} \leq min_{loss}$*)* **then**
8 break
9 **end**
10 **end**
11 return M_g

and d_c, respectively. Next, in step 6, the new data is loaded, and in step 7, we standardize the data:

$$Z = \frac{(X_u - \bar{X_u})}{\sigma_u}, \tag{2}$$

where X_u denotes the data after performing resizing, $\bar{X_u}$ is the mean value of the data, and σ_u indicates the standard deviation.

The iteration starting at step 9 denotes that the overall training process at each RBN occurs from iterations $t = 1$ to $t = T$. The parameter T can be considered as the number of time-steps during which the whole process at each RBN is executed once. In step 10, the condition for setting the switches on is checked. Therefore, after Δ time rounds, when this condition is satisfied, the software-driven contextual switch flag (cs_u) is assigned as true, and an alert is generated for turning on the physical switch. Step 14 stores the data access information for RBN u and is stored in a dedicated block ($block_u$). The local model is trained by adopting the selected hyperparameters in step 15 of Algorithm 2. Steps 16 to 21 are executed when the flag cs_u is true. In these steps, the local weight (W_u) with shallow parameters and relevant access and time-step information ($block_u$, $timestep_u$) are communicated to the cloud. Here, α denotes the deep parameter exchange ratio. The parameter $timestep_u$ holds the iteration information when the deep parameter exchange with the cloud takes place. After that, in steps 20 and 21, cs_u is set to false to prevent unauthorized transmission, and an on-display alert is generated at the RBN for the RBN manager to turn off the physical switch until the next time round commences. In the case when the cs_u flag is false, the shallow parameters of $(1 - \alpha)$ ratio from the local model (M_u) are transmitted to the cloud. Finally, after training for T time-steps, the utilized data X_u are permanently removed from the cache to enhance the security of the user's data.

Algorithm 2: Learning at the RBNs

Input : u (the current RBN), Δ (time round), T (total number of iterations), λ (deep parameter exchange rate, $0 < \lambda < 1$)

1 initialize model: $M_u \leftarrow \emptyset$
2 choose the values for hyperparameters such as epochs (η), batch-size (B), activation function (Ω)
3 initialize $timestep_u$ to 0 and send to cloud
4 $cs_u \leftarrow$ false
5 d_r, $d_c \leftarrow$ initialize data dimension
6 $X_u \leftarrow$ load new data
7 $X_u \leftarrow$ resize X_u by adopting the dimension (d_r, d_c) and then applying standardization
8 $X_u \leftarrow$ update by utilizing standardization defined in Eq. (2)
9 **for** *(*t*=1 to* T*)* **do**
10 **if** *(*t *mod* Δ*)=0* **then**
11 $cs_u \leftarrow$ true
12 generate automatic alert for turning on the physical switch
13 **end**
14 $block_u \leftarrow$ store data access information
15 $M_u \leftarrow$ update the model of RBN_u by adopting the model hyperparameters (e.g., η, B, Ω)
16 **if** cs_u*=true* **then**
17 t is assigned to $timestep_u$
18 $W_u \leftarrow$ extract local weights of λ from M_u
19 transmit W_u, $block_u$, and $timestep_u$ to the cloud
20 $cs_u \leftarrow$ false
21 generate automatic alert for turning off the physical switch
22 **else**
23 $W_u \leftarrow$ extract local weights of $(1 - \lambda)$ from M_u
24 transmit W_u to the cloud
25 **end**
26 **end**
27 delete X_u from storage

VI. Performance Evaluation

To evaluate the performance of our proposed asynchronously updating federated learning model, we use a public repository of X-ray images with COVID-19, pneumonia, and normal chest X-ray images. In contrast with the existing work dealing with small datasets, we prepared a robust dataset by merging four different existing datasets consisting of Posteroanterior (PA) chest X-rays from our earlier work [5]. Depending on the underlying AI model, two variations of the proposed asynchronously updating federated learning models are simulated based on ANN and CNN that are referred to as Fed-ANN and Fed-CNN, respectively, for brevity. Also, we define the iteration and time round for evaluating the performance of our proposal. An iteration refers to the number of times the whole process runs (e.g.,

TABLE I: Performance comparison of federated learning architectures for a varying number of users and time rounds (Learning phase).

Number of RBN	Fed-ANN				Fed-CNN			
	Time round	Iterations to converge	Accuracy	Loss	Time round	Iterations to converge	Accuracy	Loss
2	15	6	0.8968	0.0629	10	6	0.9477	0.0293
4	10	10	0.9038	0.0599	10	16	0.9456	0.0314
6	10	16	0.9157	0.0561	5	27	0.9468	0.0309
8	10	26	0.9208	0.0527	10	31	0.9444	0.03201
10	15	27	**0.9288**	0.0507	10	50	**0.9483**	0.02901

the local training for the RBNs and exchanging parameters). On the other hand, a time round consists of multiple iterations, after which the cloud is updated with the deep weights. In other words, an iteration is an atomic unit relative to the time round. For instance, if the number of iterations is 20 and the number of time rounds is 5, then for the 5th, 10th, 15th, and 20th iteration, the deep model update is triggered in our proposed approach while the shallow model parameter update takes place during the other iterations. The number of iterations was set to 20, considering the learning loss converged in all considered cases. For all the simulations, the epoch-size and batch-size were set to 50 and 16, respectively. The exponential linear unit (ELU) was employed as the activation function, while Adagrad was used as the optimizer to select and regularly update a preconditioned stochastic gradient descent smartly. For the Fed-ANN model, a fully connected layer followed by the output layer was considered. On the other hand, the Fed-CNN model consists of three convolution layers, followed by three fully connected layers and the output layer.

Table I demonstrates the comparison of Fed-ANN and Fed-CNN models for 2 to 10 users over varying time rounds during the learning phase. The Fed-ANN's best accuracy is 92.88%, which takes 27 iterations to converge, requiring 15 time rounds. On the other hand, Fed-CNN requires 50 iterations and yields a higher COVID-19 prediction accuracy (94.83%), consuming only 10 time rounds.

Fig. 3 compares the learning accuracy and loss of the Fed-ANN and Fed-CNN architectures over different time rounds varying from 5 to 20. Notice from Fig. 3a that both models' learning accuracy is over 90% at the fifth time round. Both the variations of our proposal gain higher accuracies with the increasing number of time rounds. However, the Fed-CNN model exhibits superior performance for all the time-rounds. This is also illustrated in the learning loss, in terms of the mean squared error (MSE), in Fig. 3b.

Next, the impact of iterations on the learning loss performances of Fed-ANN and Fed-CNN is investigated in Fig. 4. Both Fed-ANN and Fed-CNN demonstrate improvement in the learning with an increasing number of iterations. However, the Fed-CNN model shows a much faster convergence trend, indicating its viability as the candidate deep learning technique for the proposed federated learning framework.

In Fig. 5, we compare the required execution time and memory requirement for the training phase for the proposed Fed-ANN and Fed-CNN models. While these overheads incurred by Fed-ANN are lower than that of the Fed-CNN model during

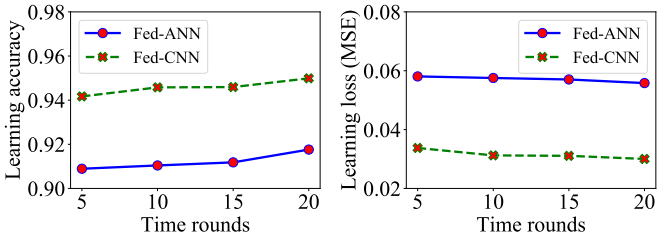

(a) Accuracy over time rounds. (b) Loss over time rounds.

Fig. 3: Learning accuracy and loss comparison of adopted federated learning architectures over different time rounds.

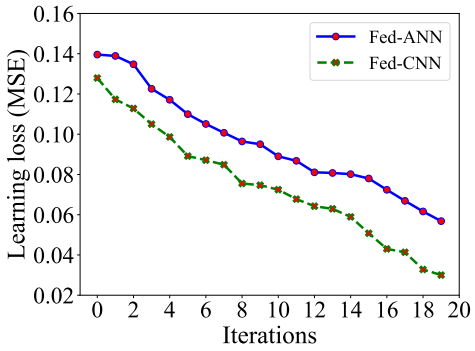

Fig. 4: The value of the loss function over growing number of iterations for the ANN and CNN-based federated learning architectures.

training, the accuracies in the inference phase between these models as well as the centralized algorithm [5] are found to be quite similar, as demonstrated in Fig. 6. Furthermore, the comparison of time required and memory consumption are shown in Fig. 7. Thus, there is a slight tradeoff between the accuracy and overhead between our proposal's two variations (i.e., Fed-ANN and Fed-CNN), which demonstrates Fed-CNN as the most suitable technique for the COVID-19 detection task.

Finally, Fig. 8 shows how our proposed asynchronous weight update method reduces the network overhead. In this case, 20 rounds are considered, which are enough to demonstrate the overhead reduction performance. Notice that with the larger deep parameter rates, a more overhead reduction is possible by performing more generic parameter exchanges from the local model using the RBN to the cloud and only transferring the specific parameters after a relatively high number of time rounds.

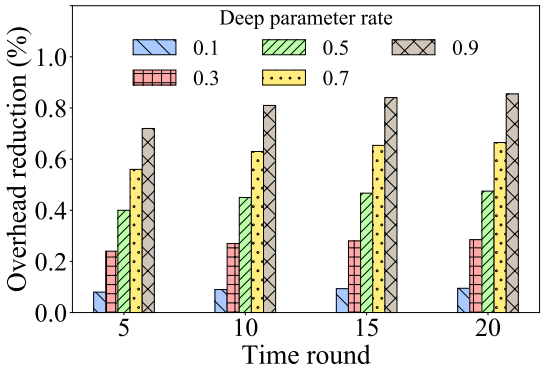

Fig. 8: Overhead reduction for the federated learning asynchronous update method over different time rounds and deep parameter exchange ratios.

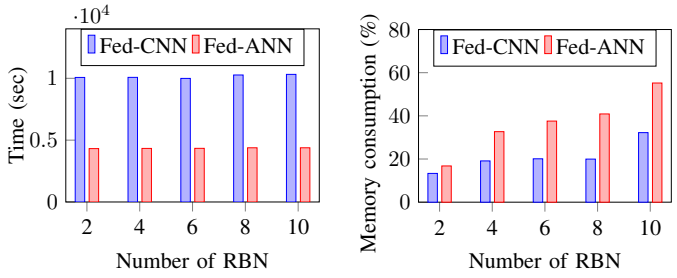

(a) Time requirement comparison. (b) Memory use comparison.

Fig. 5: Required execution time and memory consumption comparison (Learning phase).

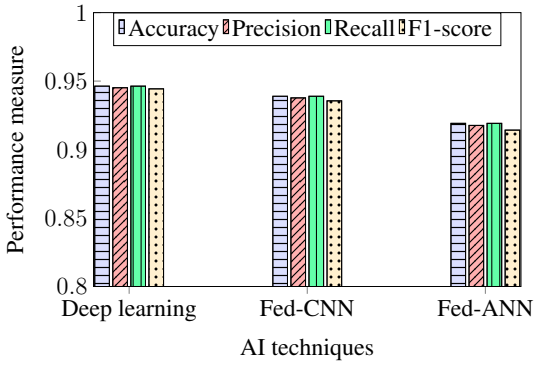

Fig. 6: Performance comparison among diverse AI methods (Inference phase).

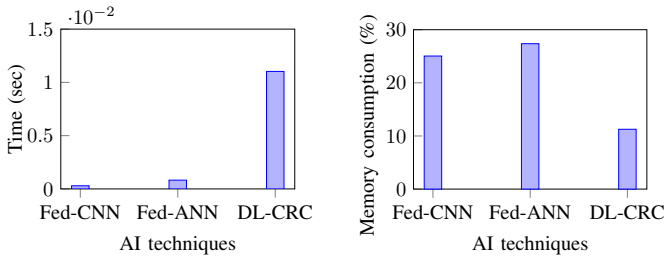

(a) Time requirement comparison. (b) Memory use comparison.

Fig. 7: Required execution time and memory consumption comparison (Inference phase).

VII. Conclusion

In this paper, we proposed an asynchronously updating federated learning model for mobile and deployable resource booth nodes to build local AI models for COVID-19 detection without the need for explicit radiograph data exchange with the cloud. This preserves the patient privacy and also alleviates the network overhead. Extensive experimental results demonstrated the viability of our proposal in terms of lightweight operation (e.g., low execution time and memory consumption) while attaining significantly high COVID-19 detection accuracy.

References

[1] S. M. A. Oteafy and H. S. Hassanein, "Leveraging tactile internet cognizance and operation via IoT and edge technologies," *Proceedings of the IEEE*, vol. 107, no. 2, pp. 364–375, Feb. 2019.

[2] F. Tariq, M. R. A. Khandaker, K. Wong, M. A. Imran, M. Bennis, and M. Debbah, "A speculative study on 6G," *arXiv preprint arXiv:1902.06700 [cs.NI]*, Aug. 2019.

[3] F. Lamberti, A. Cannavo, and P. Montuschi, "Is immersive virtual reality the ultimate interface for 3D animators?" *Computer*, vol. 53, no. 4, pp. 36–45, Apr. 2020.

[4] S. J. Adams and C. Dennie, "Chest imaging in patients with suspected COVID-19," *the Canadian Medical Association Journal (CMAJ)*, vol. 192, no. 25, pp. E676–E676, Jun. 2020.

[5] S. Sakib, T. Tazrin, M. M. Fouda, Z. M. Fadlullah, and M. Guizani, "DL-CRC: Deep learning-based chest radiograph classification for COVID-19 detection: A novel approach," *IEEE Access*, vol. 8, pp. 171 575–171 589, Sep. 2020.

[6] S. Chenthara, K. Ahmed, H. Wang, and F. Whittaker, "Security and privacy-preserving challenges of e-health solutions in cloud computing," *IEEE Access*, vol. 7, pp. 74 361–74 382, May 2019.

[7] M. Mossa-Basha, C. C. Meltzer, D. C. Kim, M. J. Tuite, K. P. Kolli, and B. S. Tan, "Radiology department preparedness for COVID-19: Radiology scientific expert review panel," *Radiology*, vol. 296, no. 2, pp. E106–E112, Mar. 2020.

[8] M. Hosseiny, S. Kooraki, A. Gholamrezanezhad, S. Reddy, and L. Myers, "Radiology perspective of coronavirus disease 2019 (COVID-19): Lessons from severe acute respiratory syndrome and middle east respiratory syndrome," *American Journal of Roentgenology*, vol. 214, Feb. 2020.

[9] "How does COVID-19 appear in the lungs?" Mar. 2020. [Online]. Available: https://www.itnonline.com/content/how-does-covid-19-appear-lungs

[10] J. Zhang et al., "Viral Pneumonia Screening on Chest X-ray Images Using Confidence-Aware Anomaly Detection," *arXiv preprint arXiv:2003.12338v3 [eess.IV]*, Sep. 2020.

[11] A. Narin, C. Kaya, and Z. Pamuk, "Automatic detection of coronavirus disease (COVID-19) using X-ray images and deep convolutional neural networks," *arXiv preprint arXiv:2003.10849v3 [eess.IV]*, Oct. 2020.

[12] A. Abbas, M. M. Abdelsamea, and M. M. Gaber, "Classification of COVID-19 in chest X-ray images using detrac deep convolutional neural network," *arXiv preprint arXiv:2003.13815v3 [eess.IV]*, May 2020.

[13] T. Ozturk, M. Talo, E. A. Yildirim, U. B. Baloglu, O. Yildirim, and U. Rajendra Acharya, "Automated detection of COVID-19 cases using deep neural networks with X-ray images," *Computers in Biology and Medicine*, vol. 121, Art. no. 103792, Jun. 2020.

[14] Z. M. Fadlullah and N. Kato, "HCP: Heterogeneous computing platform for federated learning based collaborative content caching towards 6G networks," *IEEE Transactions on Emerging Topics in Computing*, doi: 10.1109/TETC.2020.2986238.

[15] "Mobile digital radiography truck." [Online]. Available: http://www.amico.ru/en/products/digital_radiography_machines/mobile_radiography_xray_truck/

[16] M. M. School, "Radiologists publish new safety guidelines for portable X-ray units," Jan 2020. [Online]. Available: https://med.uth.edu/blog/2017/12/19/radiologists-publish-new-safety-guidelines-for-portable-x-ray-units/